Organic & Biomolecular Chemistry

Accepted Manuscript

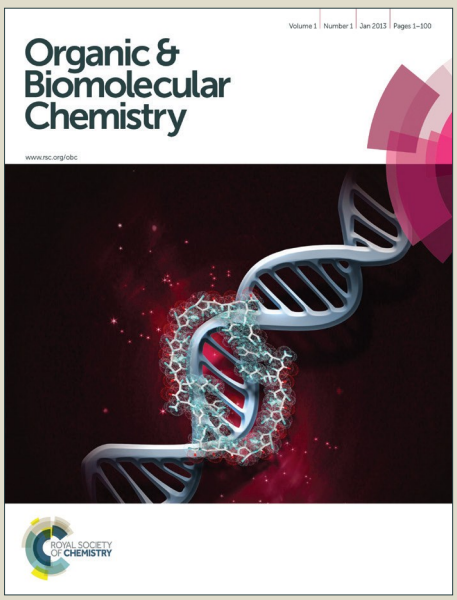

ROYAL SOCIETY OF CHEMISTRY

www.rsc.org/obc

Organic & Biomolecular Chemistry

PAPER

View Article Online
View Journal | View Issue

The Interaction of Mozobil™ with Carboxylates†

Valeria Amendola, Greta Bergamaschi, Luigi Fabbrizzi,* Maurizio Licchelli, and Carlo Mangano

Dipartimento di Chimica, Università di Pavia, viale Taramelli 12, 27100 Pavia, Italy

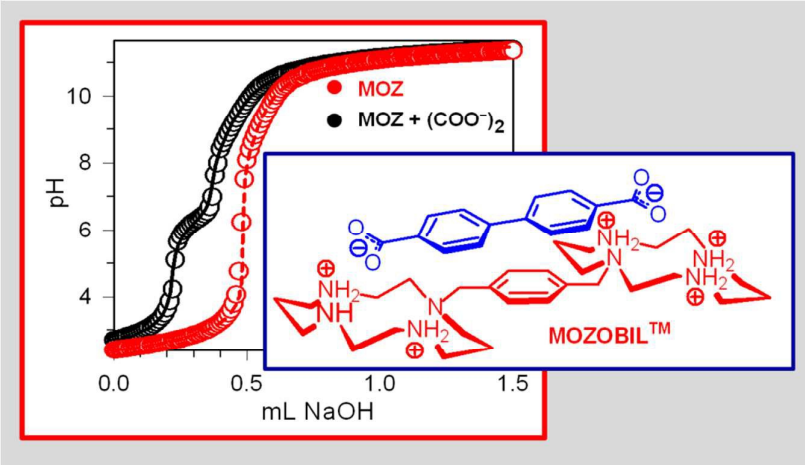

Mozobil™ interacts with linear dicarboxylates as a pentammonium cation, providing a model for binding to CXCR4 coreceptor

The Interaction of Mozobil™ with Carboxylates†

Valeria Amendola, Greta Bergamaschi, Luigi Fabbrizzi,* Maurizio Licchelli, and Carlo Mangano

Mozobil™ (1,1′-[1,4-phenylenebis(methylene)]bis[1,4,8,11-tetraazacyclotetradecane, **1**, also known as JM3100 and AMD 3100) is a specific antagonist of the chemokine coreceptor CXCR4 and favours the mobilisation from the bone marrow of stem cells, which can be used for autologous transplantation. It is believed that the interaction, of both hydrogen bonding and electrostatic nature, involves a partly protonated form of Mozobil™, LH_n^{n+} and the COO^- groups of Asp^{171} and Asp^{262} residues protruding from the walls of the pocket of the membrane protein CXCR4. We have investigated, through potentiometric titrations in 0.1 M $NaNO_3$ at 25 °C, the interaction equilibria between **1** (L) and linear dicarboxylates A^{2-}. These studies have demonstrated that the main equilibrium takes place: $LH_5^{5+} + A^{2-} \leftrightarrows [LH_5 \cdots A]^{3+}$, and that the most stable $[LH_5 \cdots A]^{3+}$ complex forms for A^{2-} = diphenyl-4,4'-dicarboxylate, whose length matches that of LH_5^{5+}. ^{1}H NMR titration experiments have shown that in the 7-10 pH interval LH_3^{3+}, LH_2^{2+} and LH^+ forms establish with diphenyl-4,4'-dicarboxylate π-π interactions, according to a topological arrangement which excludes the formation of H-bonds. It is finally suggested that, in the pocket of the CXCR4 membrane proteine, MOZOBIL™ operates as a pentammonium cation, which establishes with carboxylate groups of Asp^{171} and Asp^{262} strong interactions of hydrogen bonding and electrostatic nature.

Introduction

The octamine **1**, in which two cyclam rings have been N−N linked by a 1,4-xylyl spacer, marketed as Mozobil™ by Genzyme-Sanofi in the form of octahydrochloride,[1] is an antagonist of the CXCR4 chemokine receptor, whose major clinical use, in combination with granulocyte-colony stimulating factor (G-CSF), is the mobilisation of hematopoietic stem cells from the bone marrow into the circulating blood, for autologous transplantation.[2] In particular, a patient affected by hematological malignancies such as non-Hodgkin's lymphoma or multiple myeloma first takes the appropriate dose of Mozobil™, then is connected to an apheresis machine, which collects stem cells and returns to the body the remaining blood components. Stem cells are processed, frozen and stored. After that the patient has received the prescribed high-dose chemotherapy and/or radiation-therapy, stem cells are infused back into bloodstream. In this way, Mozobil™ has outdated and eliminated the risky and invasive surgical intervention.

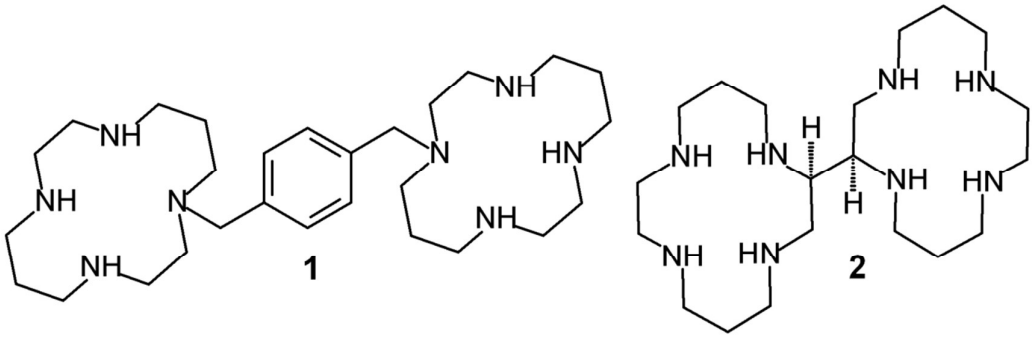

The mechanism of action is related to one of the many functions exerted by the membrane protein CXCR4,[3] that of anchoring stem cells in the bone marrow.[4] Interaction with Mozobil™ inhibits

such a function and causes mobilisation and release of stem cells to the bloodstream. It has been suggested that such an interaction has a hydrogen bonding nature, takes place in the main ligand-binding pocket of the CXCR4 receptor and involves the COO^- groups of Asp^{171} and Asp^{262} residues.[5,6] These observations prompted us to study the interaction in aqueous solution of 1 (L) with dicarboxylates.

The synthesis of the octamine **1** dates back to 1987 and its entry in pharmaceutical and clinical sciences illustrates well the role of serendipity in research.[7] This molecule was first prepared in our laboratory with a series of bicyclam analogues containing different spacers ($-CH_2CH_2-$, $-CH_2CH_2CH_2-$, $-CH_2CH_2CH_2CH_2-$, 1,3-xylyl), whose dinickel(II) complexes were obtained and electrochemically investigated for the two-step Ni^{II}-to-Ni^{III} oxidation processes, in order to evaluate mutual electrostatic effects.[8] The interest of this study was typically restricted in the area of the coordination chemistry of synthetic macrocycles. A few years later, De Clercq, testing for Johnson-Matthey the antiviral activity of $[Pt^{II}(cyclam)]^{2+}$, realised that the ligand itself, not its platinum(II) complex, exhibited inhibitory effects on the replication of human immunodeficiency virus (HIV).[7] However, such an effect was present only with the commercial cyclam obtained through the nickel(II) template synthesis by Barefield,[9] but it was totally absent with cyclam obtained by non metal-template procedures. It was then recognised that the antiviral activity was exerted by bicyclam **2** (named JM1657,[10] IC_{50} = 0.144 μM),[11] which forms as a by-product in the Ni^{II} template synthesis of cyclam,[12] and was present in traces in the commercial product. As the synthesis of **2** appeared hardly feasible and chancy, a variety of *N,N*-linked bicyclams were tested and the highest activity (much higher than for **2**) was found for **1**, isolated as octahydrochloride (JM 3100, IC_{50} = 0.005 μM).[13] When the ongoing research was transferred to AnorMED, JM3100 took the name of AMD3100. In particular, it was ascertained that the inhibitory mechanism was related to the capability of the drug **1** to prevent another function of CXCR4, that of favouring the entry of HIV into the cell. Drug **1** reached phase II clinical trials, but its development for treatment of HIV was terminated because of lacking oral availability and cardiac disturbances. In any case, studies on the HIV inhibitory effects called the attention of the scientific community on **1** and opened the route to the discovery of its valuable ability to mobilise bone marrow stem cells.[14]

The design of receptors for dicarboxylates is an important and intensely investigated topic of anion coordination chemistry, which includes polyamine cages, either partly protonated,[15,16] or containing coordinatively unsaturated transition metal ions,[17-19] and urea[20] and thiourea[21,22] derivatives.

Experimental section

Synthesis and general procedures

1,1′-[1,4-phenylenebis(methylene)]bis[1,4,8,11-tetraazacyclotetradecane (1) was synthesised according to a reported procedure.[23]

Potentiometric titrations

Potentiometric measurements were performed at 25 °C in aqueous solution (0.1 M in $NaNO_3$), with a Radiometer TitraLab 90 titration system. Titrations were performed under a dinitrogen atmosphere, in the presence of a double junction pH reference electrode (SCE) filled with aqueous $NaNO_3$ 0.1 M. Protonation constants of **1** were determined at constant ionic strength in pure water made 0.1 M in $NaNO_3$. Experiments were carried out on 10 mL of a 5×10^{-4} M solution of the polyamine, to which an excess of HNO_3 had been added. Titrations were run by addition of 10 μL

aliquots of carbonate-free standard 0.1 M NaOH, recording 80–100 points for each titration. Complexation constants were determined by carrying out a similar potentiometric titration experiment, with the additional presence in solution of 1 equiv. of the chosen carboxylate. Prior to each potentiometric titration, the standard electrochemical potential ($E°$) of the glass electrode was determined in $NaNO_3$ 0.1 M by a titration experiment according to the Gran method.[24] Titration data (pH vs. mL of NaOH) were processed with the Hyperquad® package,[25] in order to determine the equilibrium constants. When processing data on titration of a solution containing equimolar Mozobil™ and dicarboxylate, values of the stepwise dissociation constants of the dicarboxylic acid taken from literature were used and kept fixed.

^{1}H-NMR spectra in D_2O solutions at different pH values were recorded at 25 °C with a Bruker AC-400 MHz spectrometer. 1H–1H 2D correlation experiments were carried out in order to assign the signals (Fig. ESI-4 and Fig. ESI-5). All measurements were performed at 25 °C in D_2O in 0.1 M $NaNO_3$. pH ^{1}H-NMR titrations (in 0.1 M $NaCF_3SO_3$) were carried out both in the absence and in the presence of 1 equiv. of biphenyl-4,4′-dicarboxylic acid (**II**). In a typical experiment, aliquots of a 0.1M solution of CF_3SO_3H or of a solution 0.1M of NaOD in D_2O were added to a solution 5×10^{-4} M of **1**. The pH (as read by a pH electrode) was adjusted at the desired value and the ^{1}H NMR spectrum was recorded.

Results and discussion

The interaction of Mozobil™ with protons

A solution of **1** containing a known excess of acid was titrated with standard NaOH and pH was measured. The corresponding titration profiles (pH vs B/L; B/L is the ratio of mol of added NaOH over the moles of Mozobil™), experimental (red circles) and calculated (red line) are reported in Fig. 1a.

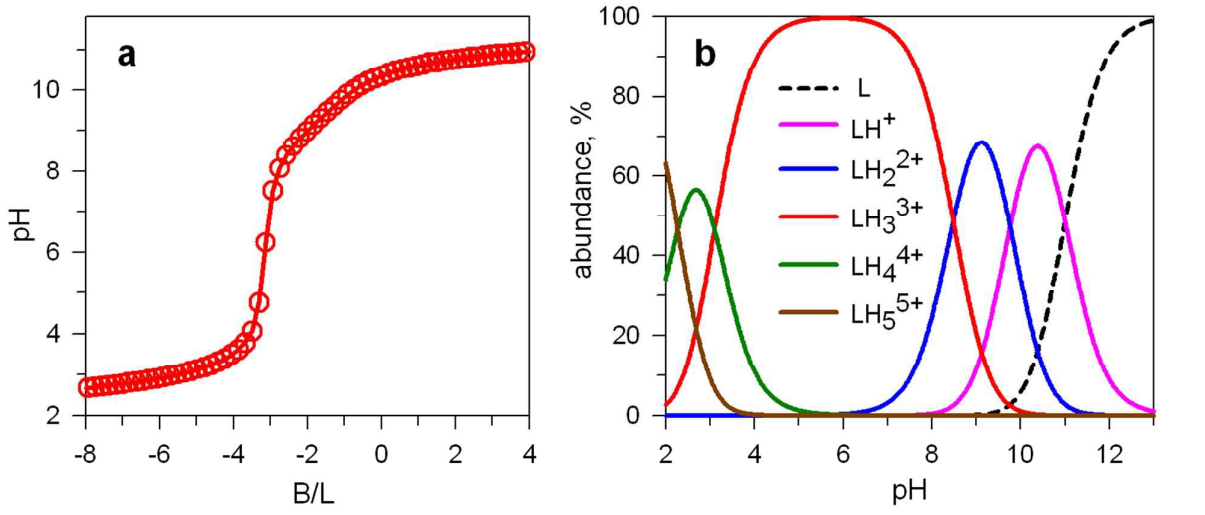

Fig. 1. (a) red symbols: titration data for a solution 7×10^{-4} of **1** in 0.1 M $NaNO_3$ at 25 °C. B/L is the ratio of mol added of base (B, NaOH) over the moles of Mozobil™ (L). Negative values in the horizontal axis refer to the neutralisation of the excess acid. Solid lines are the best fitting curves obtained through a non-linear least-squares procedure;[25] (b) distribution of the species present at the equilibrium over the 2-13 pH interval (L = **1**).

Best fitting of the titration profile, through a non-linear least-squares treatment,[25] was obtained by assuming the occurrence of five stepwise protonation equilibria, whose log *K* values are reported in Table 1. Figure 1b displays the concentrations of the species forming at varying pH over the course of the titration (% with respect to **1** = L; calculated from log *K* values in Table 1).

Table 1. Log *K* values for protonation equilibria of **1** in an aqueous solution 0.1 M $NaNO_3$ at 25 °C. In parentheses, the standard deviation on the last figure.

$L + H^+ \leftrightarrows LH^+$	11.00(1)
$LH^+ + H^+ \leftrightarrows LH_2^{2+}$	9.76(1)
$LH_2^{2+} + H^+ \leftrightarrows LH_3^{3+}$	8.48(1)
$LH_3^{3+} + H^+ \leftrightarrows LH_4^{4+}$	3.10(2)
$LH_4^{4+} + H^+ \leftrightarrows LH_5^{5+}$	2.27(2)

The ^{1}H NMR spectra of D_2O solutions of **1** (0.1 M $NaCF_3SO_3$), adjusted with triflic acid to different pH values (from 10 to 1), were also measured and are shown in Fig. 2.

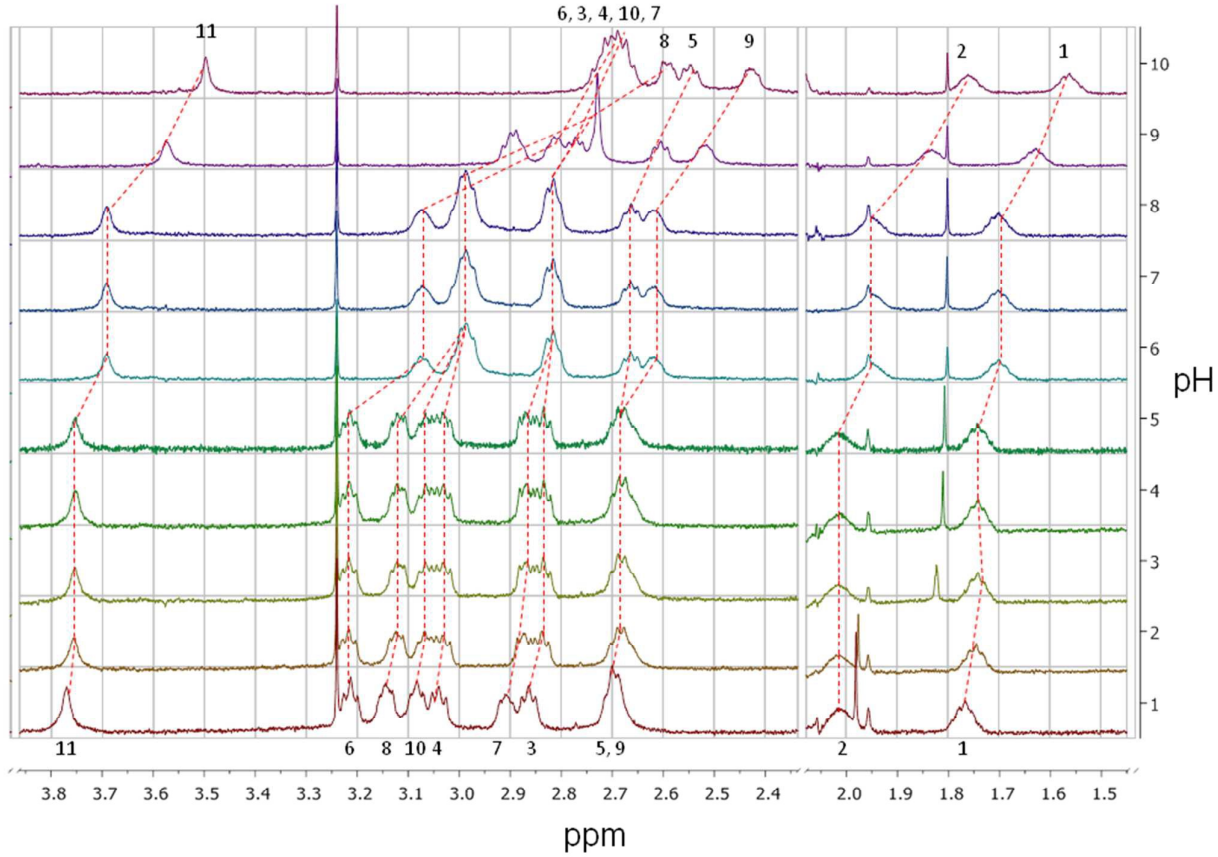

Fig. 2. ^{1}H NMR spectra of D_2O solutions 5×10^{-4} M in **1** and 0.1 M $NaNO_3$, adjusted to different pH values with triflic acid.

As a general trend, on moving from the alkaline to the acidic region, a progressive downfield shift for all C−H signals is observed. Such a behaviour is illustrated in more details for some representative signals in Fig. 3. In the same Figure, the concentrations of the species at the equilibrium at varying pH are superimposed on the diagram.

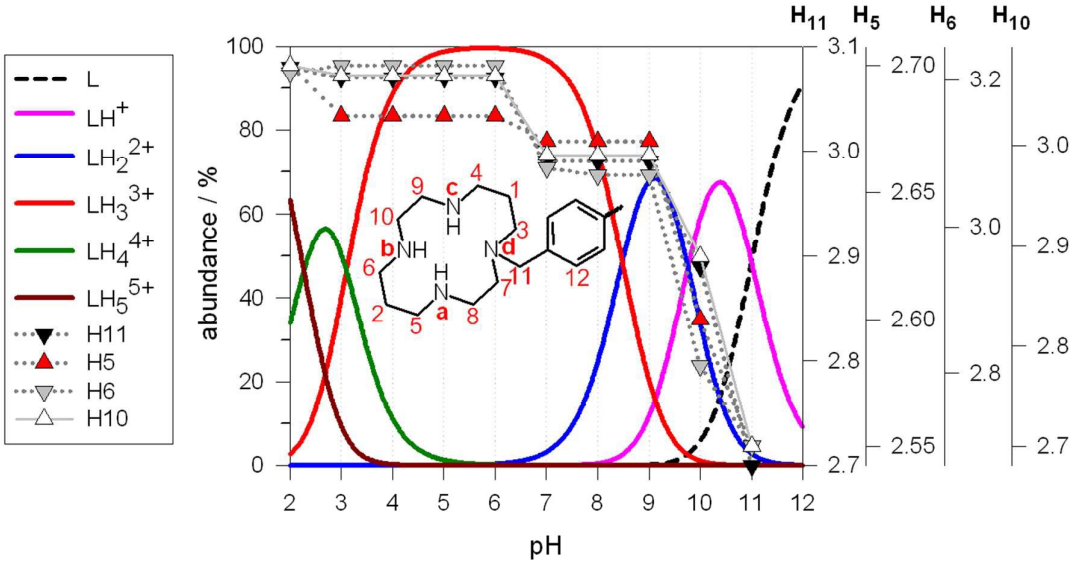

Fig. 3. Lines: concentration of the species at the equilibrium over the pH interval 2-12; symbols: chemical shifts of chosen protons measured in a D_2O solution 5×10^{-4} M in **1**.

For the considered protons a significant downfield shift δ is observed going down from pH 11 to pH 9. Below pH 9, moving to the acidic region, the downfield shift becomes much more moderate. The concentration diagram indicates that in the pH interval 11−9 LH^+ and LH_2^{2+} form. The first H^+ may bind different amine group, including the tertiary one, thus giving rise to a mixture of different isomers, a circumstance which explains the sensitivity of all C−H protons to a through-space electrostatic effect. On the other hand, in the LH_2^{2+} species repulsive electrostatic effects make ammonium groups position at the highest reciprocal distance (probably **a** and **a'**) thus giving a single rigidified species. Then, LH_3^{3+} forms, which is the dominating species until pH 4. At pH 3, with the addition of the 4th and 5th protons, a variety of C−H signals begin to undergo further downfield shift, which may suggest the formation of different positional isomers for both LH_4^{4+} and LH_5^{5+} species.

The interaction of Mozobil™ with dicarboxylates

Then, the same titration experiments were carried out for solutions containing equimolar amounts of **1** and a dicarboxylic acid.

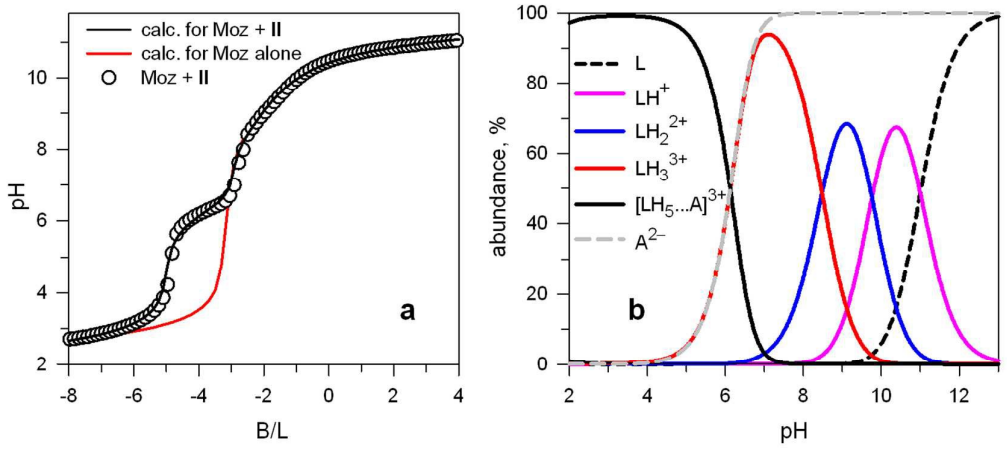

Fig. 4. (a) black circles: titration data for a solution 7×10^{-4} both in **1** and in in diphenyl-4,4'-dicarboxylic acid (**II**), 0.1 M $NaNO_3$ at 25 °C. B/L is the ratio of mol added of base (B, NaOH) over the moles of Mozobil™ (L). Negative values in the horizontal axis refer to the neutralisation of the excess acid. Solid lines are the best fitting curves obtained through a non-linear least-squares procedure;[15] (b) distribution of the species present at the equilibrium over the 2-13 pH interval.

Fig. 4a illustrates data referring to the titration in the presence of the diphenyl-4,4'-dicarboxylic acid (black circles). Best fitting of the experimental data (solid black line) was obtained by assuming the occurrence of the following additional equilibrium:

$$LH_5^{5+} + A^{2-} \leftrightarrows [LH_5 \cdots A]^{3+} \qquad (1)$$

in which A^{2-} represents the diphenyl-4,4'-dicarboxylate anion (**II**) and for which the following equilibrium constant was calculated: $\log K = 11.49 \pm 0.01$.

The $[LH_5 \cdots A]^{3+}$ species is a complex held together by hydrogen bonding (HB) and electrostatic interactions involving the pentaprotonated form of **1** and the dicarboxylate anion. A tentative structural arrangement of the complex is sketched below.

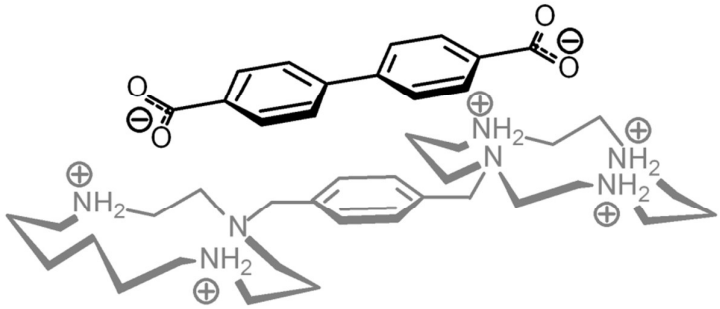

It is hypothesised that one carboxylate group establishes hydrogen bonding interactions with a doubly protonated cyclam ring, while the other carboxylate interacts with the second, tripositive cyclam subunit.

Then, ^{1}H NMR experiments were planned in order to obtain complementary information about the interaction of Mozobil™ with **II**, at varying pH. Thus, solutions 5×10^{-4} M in both **1** and the envisaged dicarboxylic acid were prepared and pH was adjusted to the desired value with triflic acid. However, to our regret, we observed the formation of a white precipitate for solutions prepared at pH < 7. Such a behaviour seems contradictory, if one considers that the potentiometric titration s had been carried out on the same *clear* solution from pH 2 to 12, on a 7×10^{-4} M concentration scale. It is possible that in the automatic potentiometric titration no time enough was left to the system under investigation to precipitate, no mechanical movements could favour nucleation of precipitate, smooth additions of the titrant (aqueous NaOH) from an automated burette caused minimal perturbation. In any case, potentiometric titration experiments were carried out on a reversible system, even if metastable, as demonstrated, for instance, by the stationary response of the glass electrode after each addition of base (typically, precipitation induces a continuous drift of the glass electrode potential).

Noticeably, at pH ≥ 7 no precipitation took place and ^{1}H NMR spectra could be recorded. Figure 5a shows the spectra taken at pH = 7 for a solution of Mozobil™ in the absence and in the presence of one equiv.of dicarboxylate.

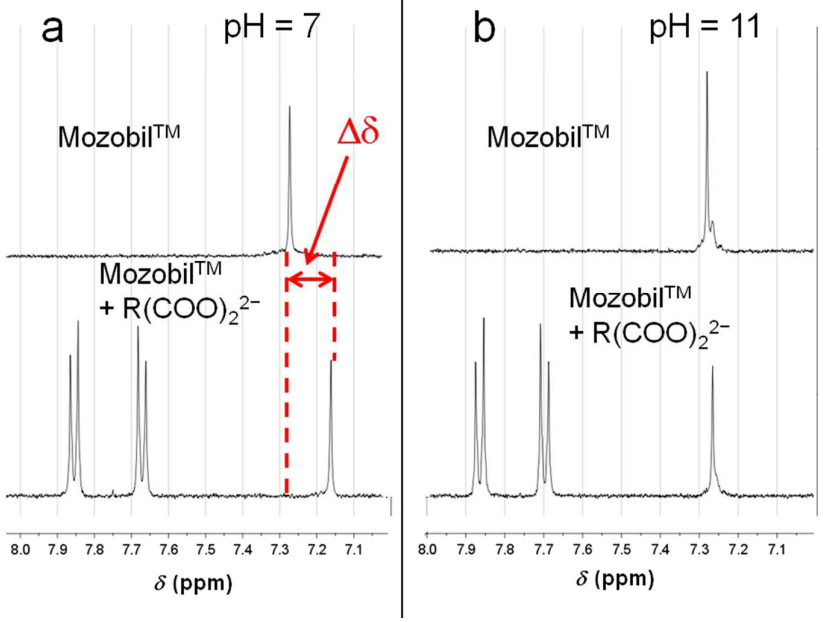

Fig. 5. ^{1}H NMR spectra taken on aqueous solutions (0.1 M $NaNO_3$) of Mozobil™ alone (upper spectra) and Mozobil™ plus 1 equiv. of **II**, at pH 7 (a) and at pH 11 (b).

On anion addition, the aromatic H12 signal undergoes a definite upfield shift, which is indicative of a π-π interaction between the diphenyl subunit of the dicarboxylate (donor) and the phenyl moiety of Mozobil™ (acceptor).

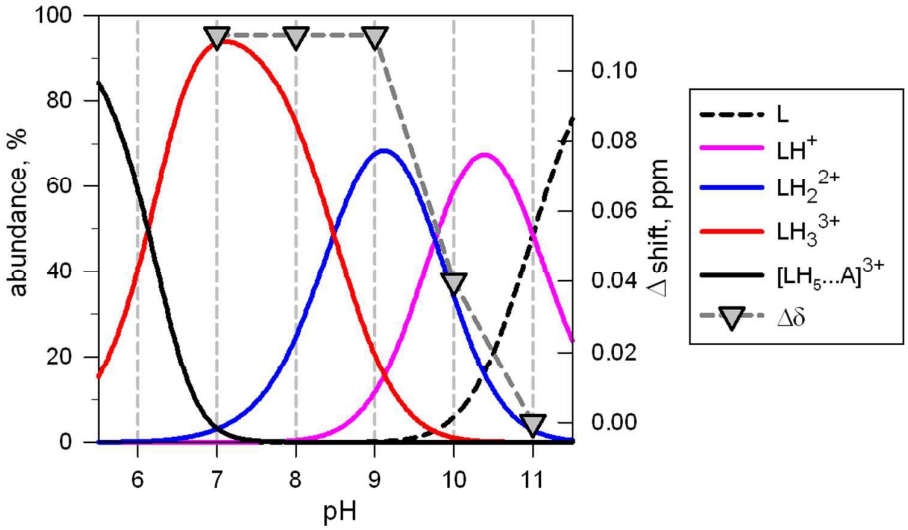

Fig.6. Symbols: Δδ difference of the chemical shifts of the aromatic proton H12 of Mozobil™ and of Mozobil™ + **II**, in solutions of different pH. Lines: concentration of the species at the equilibrium.

The same upfield shift, Δδ, is observed also for solutions adjusted to pH 8 and 9, substantially decreases at pH 10 and disappears at pH 11. Values of Δδ are plotted vs pH in Fig. 6. The concentrations of the species at the equilibrium in the same pH interval, as calculated from the potentiometric experiment, are superimposed on the same Figure.

Results are surprising: ^{1}H NMR spectra would indicate the existence of a π-π interaction between Mozobil™ and dicarboxylate in a pH interval where the hydrogen bond complex $[L\cdots A]^{3+}$ should not exist, according to potentiometric titration experiments. The puzzle can be composed if one assumes the formation of complexes $[L\cdots A]^{+}$, $[L\cdots A]$ and $[L\cdots A]^{-}$ held together by sole π-π interactions. We suggest that a structural rearrangement takes place, in which (i) the aromatic moieties of the protonated receptor and the dicarboxylate ion are placed in the most favourable positions to exert π-π donor-acceptor interaction and (ii) ammonium and carboxylate groups cannot any longer establish H-bond interactions. One could tentatively hypothesise a cross arrangement of LH_n^{n+} (n = 3, 2 , 1) and A^{2-}, which excludes any H-bond interaction and privileges π-π bonding. In this connection, it should be noted that the formation of H-bonds may disfavour the approaching of the aromatic moieties and prevent the attainment of the appropriate distance for stacking. Thus, in the $[L\cdots A]^{+}$, $[L\cdots A]$ and $[L\cdots A]^{-}$ π-π complexes, ammonium groups are not involved in any interaction and are 'sensed' by the glass electrode as in the absence of the carboxylate subunits. In fact, at pH ≥ 7 the titration curves in the absence and in the presence of dicarboxylate are coincident (see Fig. 4a), excluding any perturbation on acidic ammonium groups. In conclusion, it is hypothesised a complex system, which is present in varying topological forms differing for the nature of the interaction: hydrogen bonding from pH 2 to 7, π-π stacking from pH 7 to 10. Finally, at pH 11 the complex decomposes. This may be due to the fact that, with the formation of the neutral molecule L and disappearance of charged ammonium groups, the acidity of the acceptor phenyl group strongly decreases. As a consequence, the energy of π-π interaction becomes to low to compensate the loss of hydration energy of the two separated anion and receptor occurring during complex formation. The presence of π-π interactions in the H-bond complex $[LH_5\cdots A]^{3+}$ cannot be excluded. They may be less intense in a structural arrangement determined by hydrogen bonding. When, on pH increasing, LH_4^{4+} forms, due to the decrease of the number of ammonium groups, H-bond interactions are not strong enough to compete with π-π interactions, which strengthen as the complex rearranges to a more favourable topology.

Similar titration experiments have been carried out for dicarboxylates of different shape and size, exhibiting varying distances between the $-COO^{-}$ groups, whose formulae are reported below.

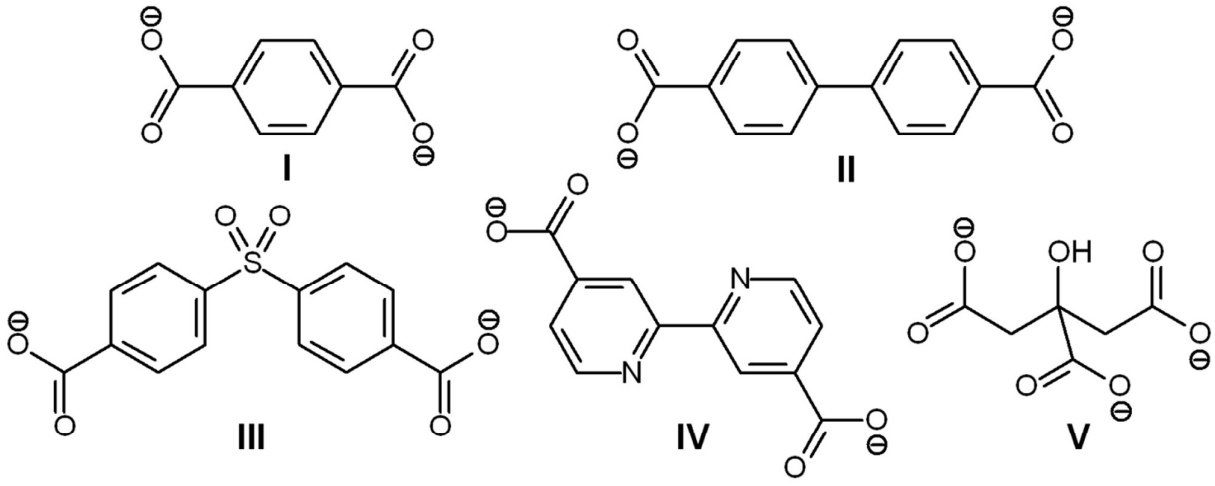

Figure 7 displays the titration profiles (pH vs B/L) for a solution containing equimolar amounts of Mozobil™, **1**, and of a dicarboxylic acid (including **II**, diphenyl-4,4'-dicarboxylic acid, whose titration profile has been previously shown in Figure 1). The scale of the horizontal axis has been

restricted to the –2 to 6 B/L range, in order to appreciate subtle differences in the profiles, to which different stabilities of the complexes correspond.

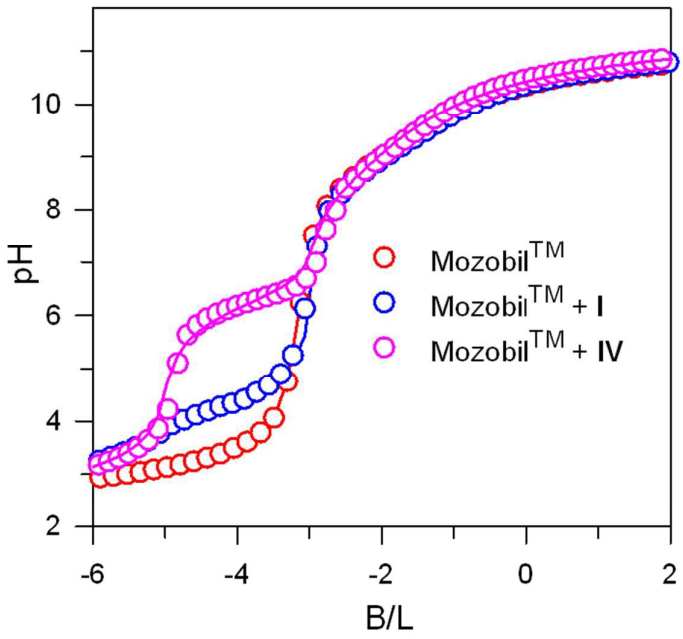

Fig. 7. Titration data for: (i) red circles: a solution of Mozobil™, **1**, in 0.1 M $NaNO_3$; (ii) symbols of different colors: solutions containing equimolar amounts of **1** and dicarboxylates **I** and **IV** in 0.1 M $NaNO_3$, at 25 °C. Solid lines are the best fitting curves obtained through a non-linear least-squares procedure.[17]

Pertinent log *K* values for equilibria of type (1), referring to the formation of H-bond complexes, were calculated through a non-linear least-squares procedure,[25] and are reported in the a bar diagram in Figure 8a.

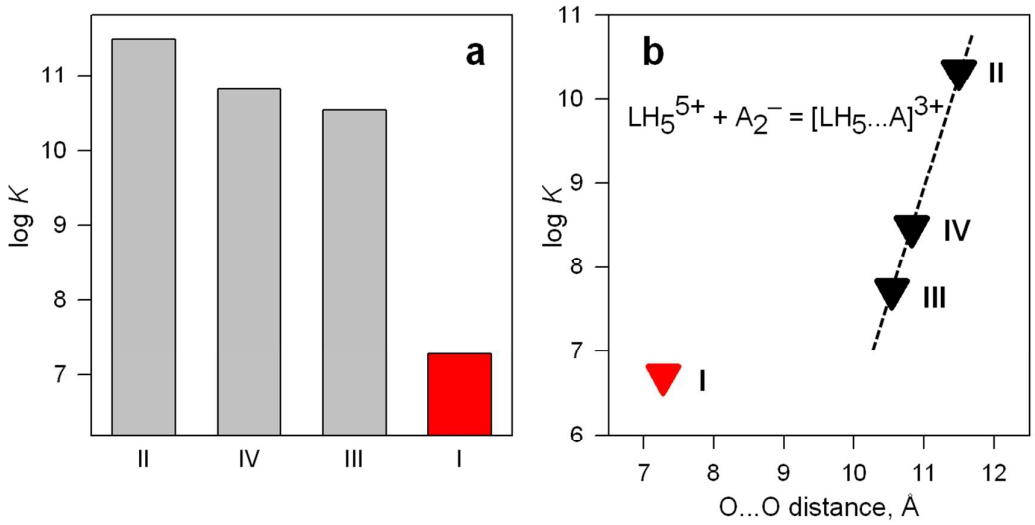

Fig. 8. (a) Log *K* values for the equilibrium: $LH_5^{5+} + A^{2-} \leftrightarrows [LH_5 \cdots A]^{3+}$ (A^{2-} = **I**–**IV**), in 0.1 M $NaNO_3$ at 25 °C; (b) plot of log *K* vs the crystallographically determined distance between the farthest oxygen atoms in dicarboxylates (**I**–**IV**).

It is suggested that the stability of the $[LH_5 \cdots A]^{3+}$ hydrogen bonding complex is related to the geometrical matching of LH_5^{5+}, positively charged H-bond donor (acid), and A^{2-}, negatively charged H-bond receptor (base). In Fig. 8b, log *K* values have been plotted vs. the distances between the farthest oxygen atoms of dicarboxylates, obtained from crystal structures (**I**: 7.3 Å;[26]

II: 11.6 Å;[27] **III**: 10.8 Å;[28] **IV**: 11.0).[29] The only crystal structure involving **1** refers to its dizinc(II) complex, [30,31] and the measured distance between the two Zn^{II} ions is 11.7 Å. It is significant that the highest stability is observed with the dicarboxylate **II**, which exhibits the closest O···O distance to 11.7 Å. As the O···O distance decreases, log *K* values diminish according to a steep straight-line (see dashed line in Fig. 8b, involving dicarboxylates **II**, **IV** and **III**). This may reflect a progressively less favourable geometrical matching between the HB donor and the HB acceptor. Dicarboxylate **I** (terephthalate) has a too short O···O distance for encompassing the two partly protonated cyclam subunits and probably establishes hydrogen bonding interactions with a single polyammonium ring. It is suggested that **II** forms the most stable H-bond complex with LH_5^{5+}, among considered linear aromatic dicarboxylates. Unfortunately, comparison could not be made with the upper homologous dicarboxylic acid, containing three linearly linked phenyl groups, [1,1':4',1"-terphenyl]-4,4" dicarboxylic acid. In fact, this acid exhibits a very low solubility in water, which prevented from any pH-metric investigation and from verifying the existence of a peak selectivity in favour of the complex of **II**. In any case, the steep slope of the log *K* vs O···O straight line in Fig. 8b discloses the dramatic effect of the geometrical correspondance of Mozobil™ and dicarboxylate on the stabilityof their complex.

The suggestion that the H-bond complex$[LH_5\cdots A]^{3+}$ represents a model, even if rather rough, for the interaction of Mozobil™ with CXCR4 may be, at a first sight, questionable. In fact, in aqueous solution, the polyammonium/dicarboxylate complex is stable in the acidic region ($2 \leq pH \leq 5$), and decomposes in a neutral solution. On the contrary, a stable interaction takes place at a physiological pH between Mozobil™ and the protruding $–COO^-$ groups of Asp^{171} and Asp^{262} residues in the pocket of CXCR4. However, a direct comparison of two events occurring one in bulk water, the other in the protein pocket is not correct, due to the extremely different nature of the two media. In particular, inside the pocket, a relatively low number of water molecules are available and the local dielectric constant is much smaller than in bulk water. From this, two important consequences derive: (i) as the two separate ions LH_5^{5+} and A^{2-} are on the overall more hydrated than $[LH_5\cdots A]^{3+}$, water molecules tend to displace the complex formation equilibrium (1) towards left. Thus, in the pocket, due to the poor availability of H_2O molecules, the relative stability of the Mozobil™/CXCR4 'H-bond complex' is expected to increase; (ii) due to the low local dielectric constant (estimated 6-7 inside the protein, 20-30 on the surface),[24] the coulombic interactions between Mozobil™ and the $–COO^-$ groups in the pocket should be especially intense, much more than in the corresponding model complex $[LH_5\cdots A]^{3+}$ in bulk water (dielectric constant 78.54 at 25 °C). Another important factor which favours the interaction inside the protein has an entropic nature: a dicarboxylate ion dispersed in the bulk aqueous solution loses translational entropy when forming a complex with Mozobil™. This entropy loss does not occur when Mozobil™ interacts with the carboxylate groups 'fixed' on the walls of the pocket. On these bases, it is suggested that Mozobil™, in its pentaprotonated form $[LH_5]^{5+}$, forms a 'complex' with $–COO^-$ residues of Asp^{171} and Asp^{262}, whose stability results from a variety of concurring factors. Establishing of π-π in the pocket seems to be excluded for (i) the unavailabily of properly oriented aromatic subunits from the walls of the pocket, and (ii) the formation of relatively strong hydrogen bonding interactions between LH_5^{5+} and the protruding carboxylates.

It has to be noted that titration of **1** in the presence of 1 equiv. of citrate (**V**), in 0.1 M $NaNO_3$ is coincident with the profile of the titration of **1** alone, ruling out the formation of a complex. This may be surprising, if one considers that the citrate ion shows an O···O distance (7.2 Å)[33] comparable to that of terephthalate (**I**, 7.3 Å) and, in addition, possesses 3 negative charges. The instability of

the Mozobil™/citrate complex can be ascribed to the absence of π-π interaction, if any. Most probably, failure in complex formation should be ascribed to lack of shape matching and to the flexibility of citrate compared to the more rigid dicarboxylates containing aromatic spacers.

Conclusion

Equilibrium studies in aqueous solution have shown that Mozobil™ interacts with linear dicarboxylates in its pentaprotonated form to give a 1:1 complex, $[LH_5\cdots A]^{3+}$, held together by hydrogen bonding and electrostatic interactions. At pH ≥ 7 hydrogen bonding interactions vanish, but Mozobil™ and dicarboxylate are still held together by π-π interactions, giving rise to complexes of different topology: $[LH_3\cdots A]^{+}$, $[LH_2\cdots A]$, $[LH\cdots A]^{-}$. It is suggested that the H-bond complex $[LH_5\cdots A]^{3+}$ can provide a reasonable model for the interaction of Mozobil™ in the pocket of the CXCR4 protein, involving the drug in the form of a pentammonium cation and the protruding carboxylate groups. In particular, such an interaction is expected to occur in spite of the neutral pH, for two main reasons: (i) the limited number of water molecules favours a process characterised by a decrease of the electrical charges (+ 5 – 2 = + 3) (ii) the low value of the local dielectric constant makes the electrostatic contribution to the complex formation more important. 'Fixedness' of the carboxylate residues inside the pocket provides an additional contribution to the stability, of entropic origin.

This work has demonstrated that a rod-like shaped molecular system of the length of ~ 12 Å, possessing a double positive charge at one end and a triply positive charge at the other, can behave as an efficient antagonist of CXCR4 coreceptor, with related beneficial therapeutic and clinical consequences. Perhaps, chemical ingenuity can suggest a route different from that of bicyclams.

Dipartimento di Chimica, Università di Pavia, viale Taramelli 12, 27100 Pavia, Italy

† Electronic supplementary information (ESI) available: details on the synthesis of Mozobil™. Distribution diagram (abundance vs pH) for Mozobil™/dicarboxylate complexes. COSY spectra of D_2O solutions of **1** at pH 2 and pH 10.

Acknowledgements

This research was supported by the Italian Ministry of University and Research (Project PRIN: InfoChem).

Notes and references

(1) http://www.mozobil.com/

(2) W. C. Liles, H. E. Broxmeyer, E. Rodger, B. Wood, K. Hübel, S. Cooper, G. Hangoc, G. J. Bridger, G. W. Henson, G. Calandra, D. C. Dale, *Blood*, 2003, **102** (8), 2728−2730.

(3) V. Saini, A. Marchese, M. Majetschak, *J. Biol. Chem.,* 2010, **285** (20), 15566–15576..

(4) M. P. Rettig, G. Ansstas, J. F. DiPersio, *Leukemia*, 2012, **26**, 34–53

(5) L. O. Gerlach, R. Skerlj, G. J. Bridger, T. W. Schwartz, *J. Biol. Chem.,* 2001, **276** (17), 14153–14160.

(6) S. Hatse, K. Princen, L.-O. Gerlach, G. Bridger, G. Henson, E. De Clercq, T. W. Schwartz, D. Schols, *Mol Pharmacol.*, 2001, **60** (1),164–173.

(7) E. De Clercq, *Biochem. Pharmacol.*, 2009, **77**, 1655−1664.

(8) M. Ciampolini, L. Fabbrizzi, A. Perotti, A. Poggi, B. Seghi, F. Zanobini, *Inorg. Chem.* 1987, **26** (21), 3527–3533.

(9) E. K. Barefield, F. Wagner, A. W. Herlinger, A. R. Dahl, *Inorg. Synth.*, 1976, **16,** 220−225.

(10) E. De Clercq, N. Yamamoto, R. Pauwels, M. Baba, D. Schols, H. Nakashima, J. Balzarini, Z. Debyser, B. A. Murrer, D. Schwartz, D. Thornton, G. Bridger, S. Fricker, G. Henson, M. Abrams, D. Picker, *Proc. Natl. Acad. Sci. USA*, 1992, **89** (12), 5286–5290.

(11) Inhibition to the replication of various HIV-1 strains in various human T-cell systems. Compare to cyclam: IC_{50} = 399 μM.

(12) E. K. Barefield, D. Chueng, D. G. Van Derveer, F. Wagner, *J. Chem. Soc., Chem. Comm.*, **1981**, 302−304.

(13) E. De Clercq, N. Yamamoto, R. Pauwels, J. Balzarini, M. Witvrouw, K. De Vreese, Z. Debyser, B. Rosenwirth, P. Peichl, R. Datema, D. Thornton, R. Skerlj, F. Gaul, S.; Padmanabhan, G. Bridger, G. Henson, M. Abrams, *Antimicrob. Agents Chemother.*, 1994, **38** (4), 668–674.

(14) E. De Clercq, *Pharmacol. Ther.*, 2010, **128** (3), 509−518.

(15) B. Dietrich, J. Guilhem, J.-M. Lehn, C. Pascard, E. Sonveaux, *Helv. Chim. Acta,* 1984, **67**, 91−104.

(16) J.-M. Lehn, R. Meric, J.-P. Vigneron, I. Bkouche-Waksman, C. Pascard, *J. Chem. Soc. Chem. Commun.*, 1991, 62−64.

(17) M. Boiocchi, M. Bonizzoni, L. Fabbrizzi, G. Piovani, A. Taglietti, *Angew. Chem., Int. Ed.*, 2004, **43**, 3847−3852.

(18) P. Mateus, R. Delgado, V. André, M. T. Duarte, *Inorg. Chem.*, 2015, **54** (1), 229–240.

(19) G. Alibrandi, V. Amendola, G. Bergamaschi, L. Fabbrizzi, M. Licchelli, *Org. Biomol. Chem.***,** 2015,**13**, 3510−3524.

(20) B. R. Linton, M. . Goodman, E. Fan, S. A. van Arman, A. D. Hamilton, *J. Org. Chem.*, 2001, **66** (22), 7313–7319.

(21) A. J. Lowe, F. M. Pfeffer, *Org. Biomol. Chem.*, 2009, **7**, 4233–42.

(22) A. J. Lowe, B. M. Long, F. M. Pfeffer, *J. Org. Chem.*, 2012, **77**, 8507−8517.

(23) M. Achmatowicz, L. S. Hegedus, *J. Org. Chem.*, 2003, **68** (16), 6435−6436.

(24) P. Gans, B. O'Sullivan, *Talanta*, 2000, **51** (1), 33–37.

(25) Hyperquad® package; Gans, P.; Sabatini, A.; Vacca, A. *Talanta*, 1996, **43**, 1739–1753; http://www.hyperquad.co.uk/index.htm; accessed 27 July, 2015.

(26) A. Lemmerer, *Cryst. Growth Des.*, 2011, **11** (2), 583−593; U. K. Das, P. Dastidar, *Cryst. Growth Des.*, 2013, **13** (10), 4559−4570; D.-M. Xie, C.-X. Chen, H.-X. Chen, H.-B. Wang, *Acta Crystallogr., Sect. E: Struct. Rep. Online*, 2010, **66** (pt 8), o2074.

(27) T. Okuno, Y, Sakoda, T. Kinuta, T. Sato, H. Tokutome, N. Tajima, Y. Nakano, M. Fujiki, R. Kuroda, Y. Imai, *Cryst. Eng. Comm.*, 2012, **14**, 4819−4825; T. Yuge, M. Miyata, N. Tohnai, *Cryst. Growth Des.*, 2006, **6**, 1271−1273.

(28) C.-J. Wang, Y.-Y. Wang, J.-Q.Liu, H. Wang, Q.-Z. Shi, S.-M. Peng, *Inorg. Chim.Acta*, 2009, **362** (2), 543−550; G. Smith, U. D. Wermuth, *Acta Crystallogr., Sect. E: Struct. Rep.Online*, 2011, **67** (Pt 11), o2966.

(29) T. T. Cao, Y. Ma, C. Yang, D.-Z. Liao, S.-P. Yan, *J. Coord. Chem.*, 2010, **63**, 3093−3100; T. Fujihara, A. Kobayashi, A. Nagasawa, *Acta Crystallogr., Sect.E: Struct. Rep. Online*, 2004, **60** (Pt 2), o353-o355.

(30) X. Liang, J. A. Parkinson, S. Parsons, M. Weishäupl, R. O. Gould, S. J. Paisey, H. Park, T. M. Hunter, C. A. Blindauer, S. Parsons, P. J. Sadler, *J. Am. Chem. Soc.*, 2002, **124** (31), 9105−9112.

(32) X. Liang, P. J. Sadler, *Chem. Soc. Rev.*, 2004, **33**, 246−266.

(33) L. Li, C. Li, Z. Zhang , E. Alexov, *Chem. Theory Comput.*, 2013, **9** (4), 2126–2136.

(34) A. Fischer, G. Palladino, *Acta Crystallogr.,Sect. E: Struct. Rep. Online*, 2003, **59** (Pt 11), m1080−m1082; M. Rossi, L. F. Rickles, L. F. Glusker, *Acta Crystallogr., Sect. C: Cryst. Struct. Commun.*, 1983, **39** (Pt 8), 987−990.